



Brain Tumor Detection Using a Broadband Microstrip Antenna with a Defected Ground Structure

Laila T. Rakha, Nihal F.F Areed* and Hamdi A. El-Mikati

Citation: Rakia , L.; Areed, N.; El-Mikati, H. *Inter. Jour. of Telecommunications, IJT* 2022, Vol. 02, Issue 02, pp. 1-13, January 2022. https://ijt.journals.ekb.eg/article_266292.html

Editor-in-Chief: Youssef Fayad

Received: 2022-08-25.

Accepted: 2022-10-05.

Published: 2022-10-19

Publisher's Note: The International Journal of Telecommunications, IJT, stays neutral regarding jurisdictional claims in published maps and institutional affiliations.



Copyright: © 2022 by the authors. Submitted for possible open access publication under the terms and conditions of the International Journal of Telecommunications, , Air Defense College, ADC, <https://ijt.journals.ekb.eg/>

¹Mansoura University Electronics and Communication Engineering Department, Faculty of Engineering, Mansoura University, Mansoura 35516 Egypt
lailarakha67@gmail.com, nahoolaf@mans.edu.eg, h.elmikati@gmail.com

Abstract: Brain tumors is a common cause of death worldwide. It may be difficult to detect a brain tumor at an early stage due to its small size as well as some other drawbacks of the methods used for detection. In this paper, a proposed rectangular microstrip patch antenna with Defect Ground Structure (DGS) operating in the X-band around 5 GHz was developed for tumor detection. The antenna was designed with dimensions of 23.72×29.78×1.588 mm³ and a Roger-RT/5880 ($\epsilon_r=2.2$) substrate material and a rectangular feed-line was used to supply the antenna's radiating patch. The design dealt with a single element and an array of elements in order to improve performance compared to previously published research. The antenna's effectiveness was evaluated by applying it to a brain phantom with and without a tumor. The dimensions of the antennas are optimised to effectively identify different localized tumours with a minimum radius of 5 mm while also taking into account special safety issues to be less than 1.6 W/Kg for a 1g cube-shaped tissue.

Keywords: Brain tumor, Microstrip Antenna, DGS, Return loss, Gain, SAR

1. Introduction

According to the World Health Organization, cancer has just surpassed cardiovascular disease as the second leading cause of death worldwide, killing 9.6 million people annually (WHO). According to the symptoms, there are many different types of cancer, and brain cancer is one of them. A rare and varied group of malignancies are the cancers of the brain and central nervous system. These tumor types account for 3 percent of cancer cases and are more common in men than in women. Brain cancer is among the 10 most lethal cancers, while having a low incidence rate [1]. The tumor's size, location, and stage of development are its defining characteristics [2]. Tumors come in two different varieties: benign and malignant. The tumor that does not contain any malignant cells and is not particularly dangerous is called benign [3]. A malignant tumor, on the other hand, is the growth of cancerous cells and is regarded as fatal, dangerous, and unpredictable. Additionally, it spreads fast to the nearby tissue and significantly impairs each tissue's ability to perform its particular activities [2].

It is possible to find brain tumors or cancerous cells in the brain using a variety of methods, including X-ray mammography, magnetic resonance imaging (MRI), ultrasound, radiography, computed tomography (CT scan). However, each of these methods has certain limitations, such as high ionizing radiation levels and the inability to distinguish between benign and malignant tumors in some cases. The antennas have a significant

impact on the end result's quality and image performance. An antenna for one of these systems should be able to meet a number of criteria, including ease of integration, compactness, a simple geometrical structure, a wide bandwidth, and a high gain. Microstrip Patch Antennas (MPAs) can meet these needs. It features a flat shape, a low profile, a modest weight, and a small volume. It has a planar shape, a low profile, a small weight, a small volume, and a low fabrication cost, among other features.

Recently, Defect Ground Structure (DGS) is an intentionally created slots in the ground plane of a MPA structure to enhance its performance. Such Defects are introduced to reduce harmonics, suppress mutual coupling, and improve bandwidth [4-6]. Microwave Imaging (MI) employing a MPA with DGS is one of the most recent successful created approaches for identifying the brain tumor. The dielectric properties (such as permittivity, conductivity) of the stable cells and tumor-affected cells of the human brain are what determine how the Microwave Imaging (MI) system functions [7-9]. In order to irradiate the human head under inspection with microwave energy, MPA is a crucial component of microwave imaging systems [10-17]. To make a more accurate diagnosis, key microstrip patch antenna performance measures, such as Specific Absorption Rate (SAR), Return loss (S_{11}), Radiation Pattern, directivity, and polarization, need to be thoroughly assessed [8].

By building on earlier research, this work aims to create a MPA that can detect brain cancer. The antenna's operating frequency is equal to 5 GHz. The antenna was designed with dimensions of $23.72 \times 29.78 \times 1.588 \text{ mm}^3$ and a Roger-RT /5880 substrate material with dielectric constant of 2.2. The antenna's radiating patch was supplied by a rectangular feed-line. The antenna's effectiveness was tested on a brain phantom with and without a tumor. The antenna dimensions are optimized to effectively identify different localized tumors with a minimum radius of 5 mm while also taking special safety issues into account to be less than 1.6 W/Kg for a 1g cube-shaped tissue [13-16]. There are five sections to this study. Following the introduction portion, section 2 describes the suggested design. The parametric study and simulation results for the MPA array are presented in Section 3. In addition, the proposed antenna's applicability for Brain tumor detection is discussed in section 4. Lastly, Section 5 presented the work's conclusion.

2. Proposed Design

The top and bottom schematics for the proposed MPA array are shown in Figure 1 (a) and (b). The antenna was created in stages. It begins with a single-element, then the analysis is extended to a two and 4-element array, and lastly to four-element arrays. Figure 1 depicts the proposed antenna with optimal dimensions.

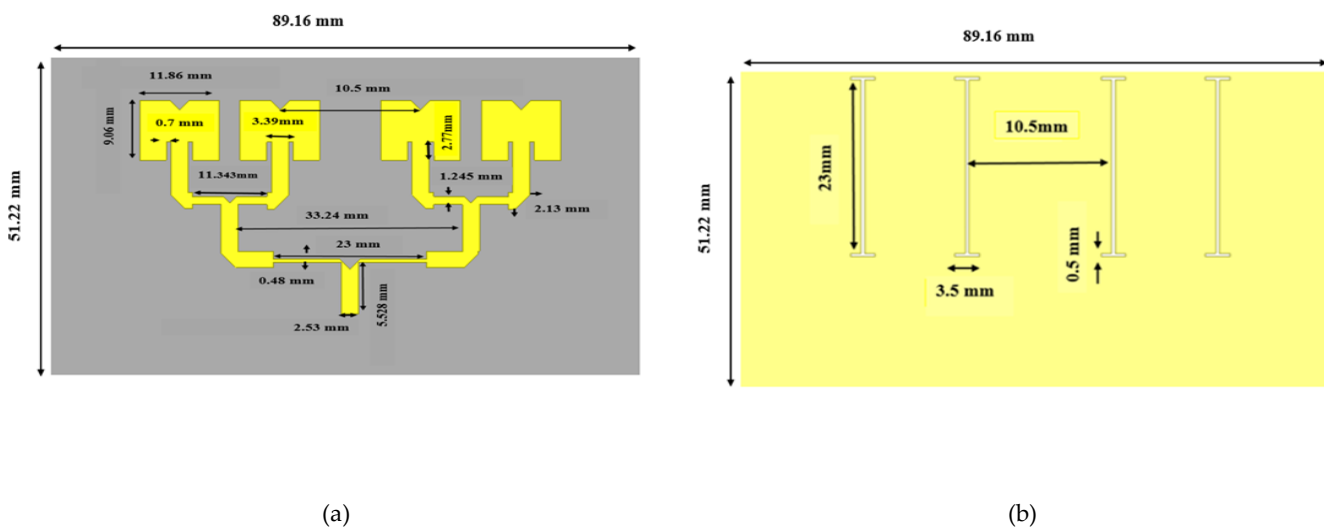


Figure 1. The proposed antenna configuration: (a) top view, (b) bottom view

The inset-fed method is utilized to create a single patch on a Rogers RT/ Duroid 5880 (tm) substrate with a dielectric constant (ϵ_r) of 2.2 and a loss tangent of 0.009, as shown in Fig.2. The dimensions of the substrate are calculated to be 27.3 and 28.7 mm. The substrate thickness is taken by 1.588 mm. The patch dimensions are set to 9.06 mm \times 11.86 mm. The rectangular patch antenna design equations [4-6] were used to get the dimension. The DGS and slotted patches are employed to enhance the design performance.

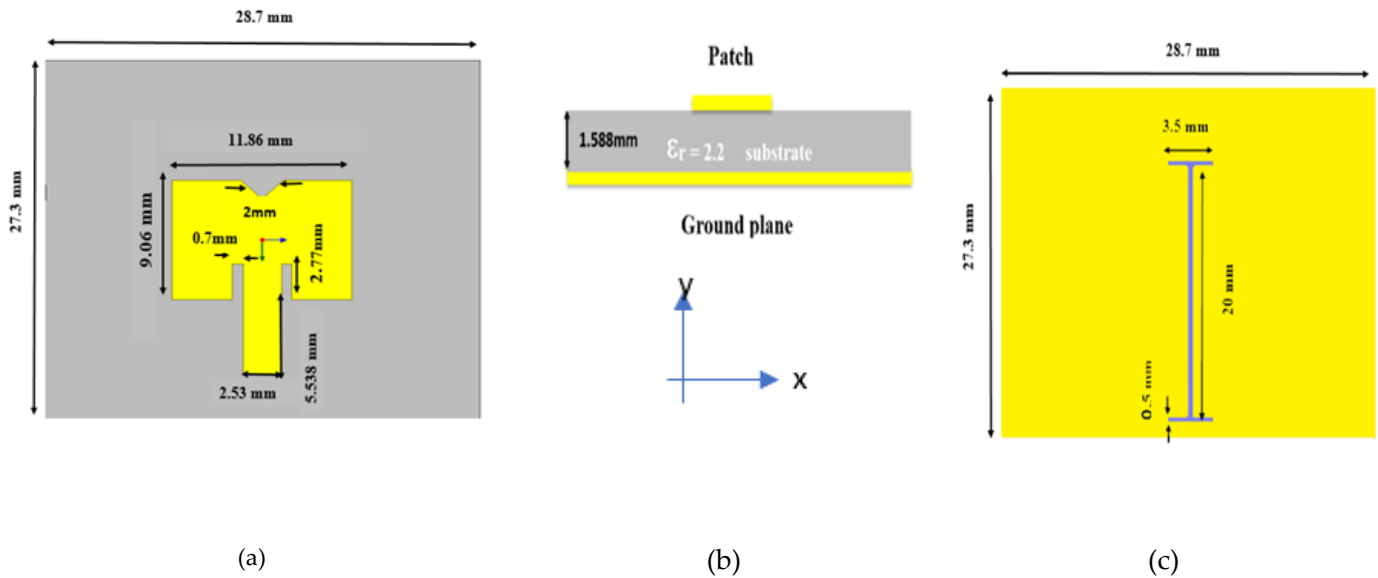


Figure 2. Proposed single patch design (a) top view, (b) side view, (c) bottom view

To tune the frequency around 10 GHz and improve performance, the ground plane and the patch have been defected with an I-shaped hole and a triangle-shaped hole, respectively. The width of the I-slot along the x and y axes is 0.5 mm and 20 mm, respectively. The I-slot hole is loaded from two sides by an extra inset of size 3.5 mm \times 0.5 mm. Further, a triangle-shaped hole with a base of 2 mm has been etched on the top edge of the patch. The dimensions of the etched holes have been selected after many trials to maintain the operating frequency around 10 GHz with optimised performance. Next, a two-element array antenna has been implemented as shown in Fig.3. In the considered design, the spacing between patches is tuned as far as $\lambda/2$ (15 mm) to avoid mutual coupling.

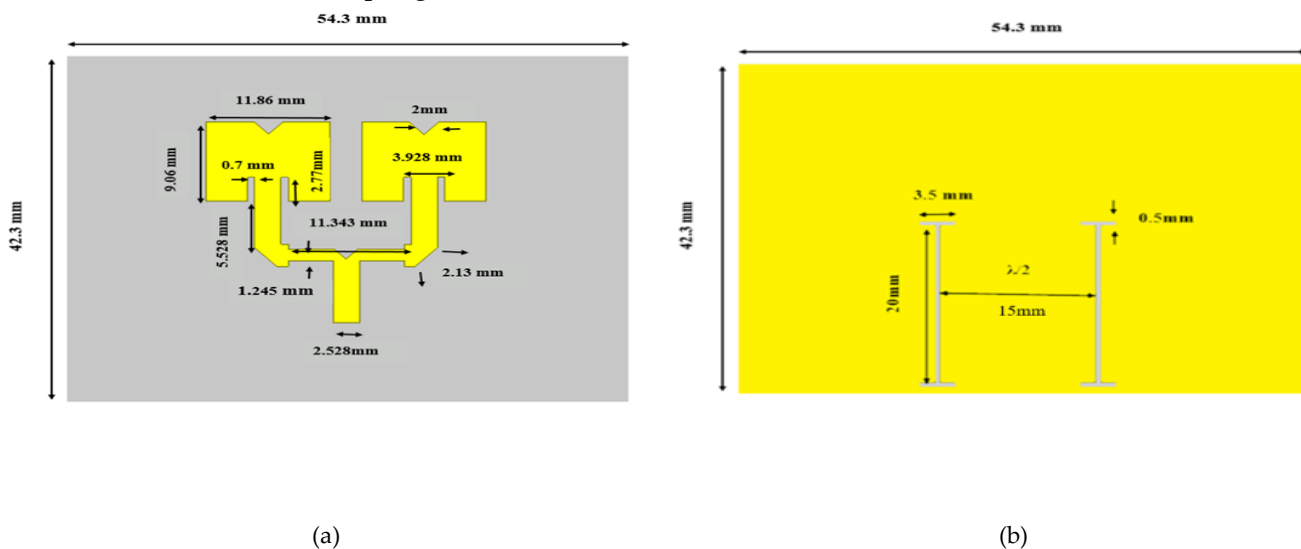


Figure 3. Proposed two element arrays: (a) top view, (b) bottom view.

The width of the hole along the Y-axis is 0.5 mm and the length of the hole along the x-axis is 20 mm. Each I-shape hole is etched underneath the transmission line patch plane. The optimum dimensions of the design have been calculated after a parametric study. Further, the transmission lines are not usually in a straight line in several feed networks, but they are in a straight line in several feed networks. They're thought to fold up to some extent. When a horizontal transmission line is folded into a vertical transmission line 90, the majority of the power from the input is reflected back at the discontinuity towards the source, lowering the system's performance since it causes a change in the line's capacitance and thereby affects the line's impedance. The mitered-bended approach was utilized in the antenna design to reduce transmission line losses. The purpose of the mitered bend is to remove that small amount of capacitance, restoring the line's impedance to the matching impedance. Figure 4 depicts the structure of the microstrip mitered bend that was used to address these concerns. The dimension of the truncation channel (x) may be computed using the diagonal of a square bend; D. The dimensions of the bens can be calculated with the aid of the following equations [4-6].

$$D = W \times \sqrt{2} \quad (1)$$

$$X = D \times \left(0.52 + 0.65e^{(-1.35 \times \frac{W}{h})} \right) \quad (2)$$

$$A = \left[X - \frac{D}{2} \right] \times \sqrt{2} \quad (3)$$

w is the width of the transmission line and is equal to 2.53 mm, $D = 3.578$. We choose a matching impedance of 75 and the length of the transmission line is 5.67 mm. X and A calculated by the above equations read 2.13 mm and 0.48 mm; respectively.

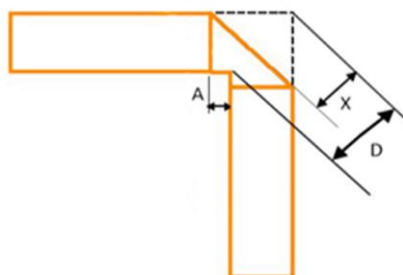


Figure 4 Microstrip Mitered bend [4].

3. Simulation Results

The proposed design's performance has been measured using the Finite Element Method (FEM). Surface current distribution, reflection coefficient, gain, and radiation patterns are among the derived metrics. The computed surface current distributions for arrays with and without DGS are shown in Figure 5. As shown in the graph, DGS has a significant impact on the surface current distribution. The surface current is more concentrated in the feeder portion, where there are ground holes. Furthermore, the surface current on the ground plane has been radically altered as a result of the I-shaped holes under the patch and feeder. The proposed microstrip antenna features two equivalent electric current sources in this scenario, with the patch current and DGS current resonating at dual frequencies. On the other hand, using a 4-element array enhances the matching, gain, and directivity, as evident from the S_{11} curves and radiation pattern calculations shown in Fig.6 (a) and (b), respectively. In detail, using a 4-element array results in the increment of the 10-dB bandwidth from 700MHz to 1200MHz and gain from 8 dB to 13 dB and minimizes the half-power beam width to be 33.6 instead of 77.4 in comparison with a single patch.

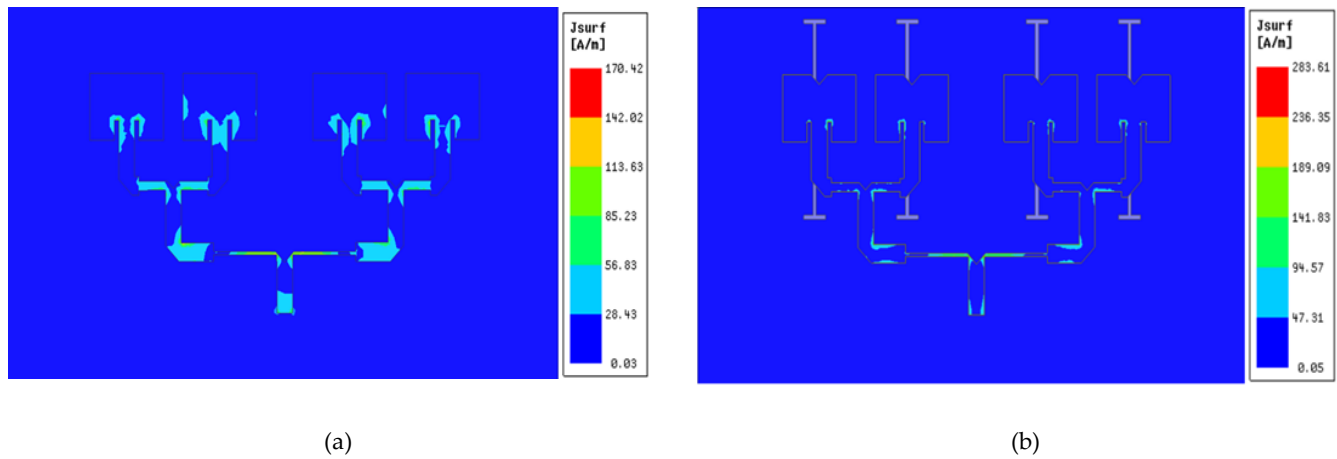


Figure 5. Surface current distributions: (a) the proposed design without slots, (b) the proposed design with slots in patch and ground plane at 10 GHz.

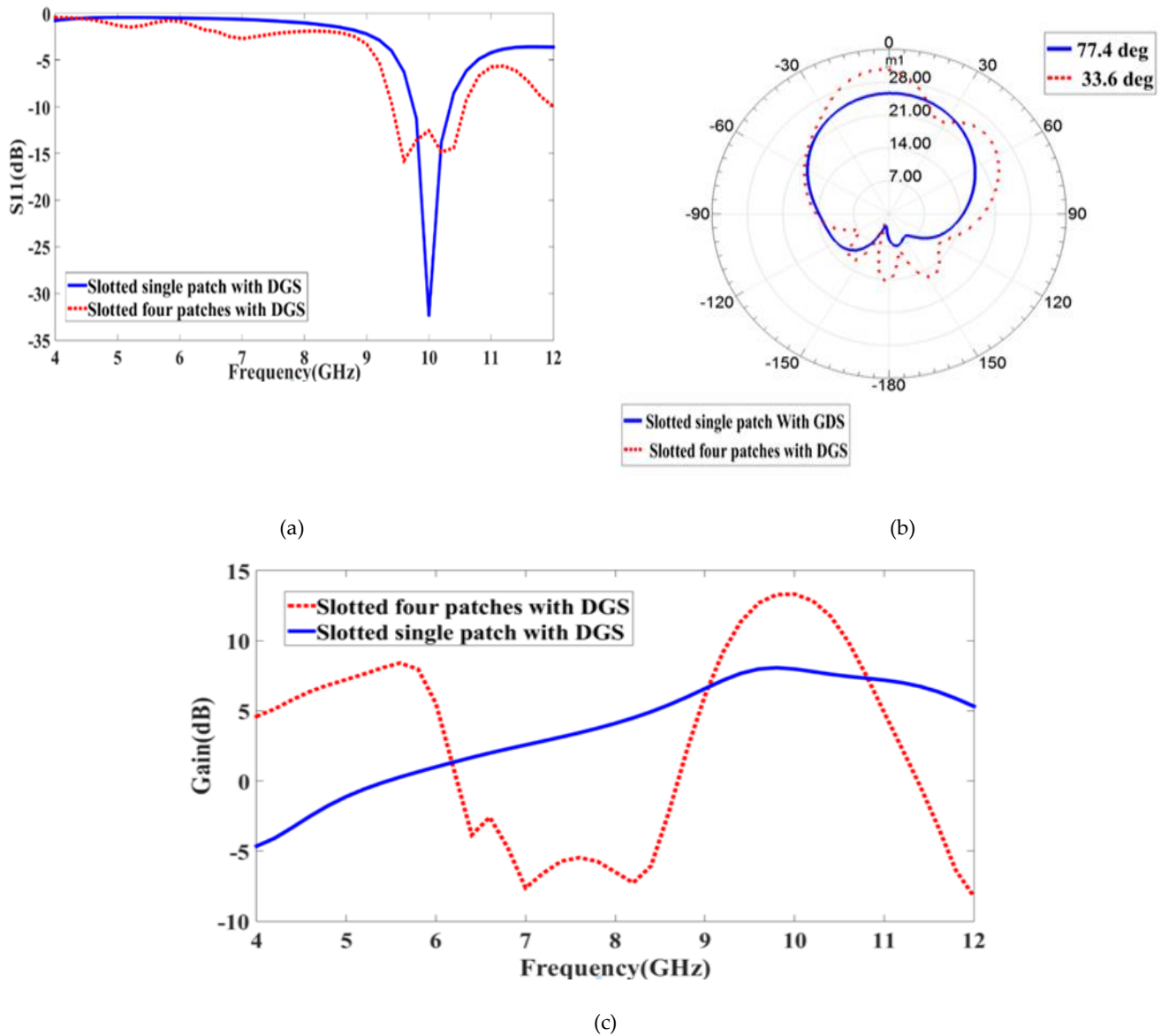
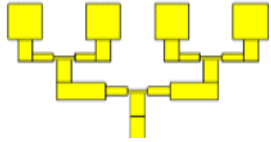
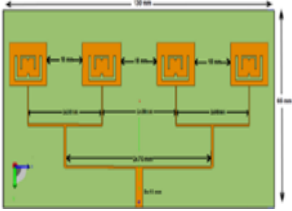
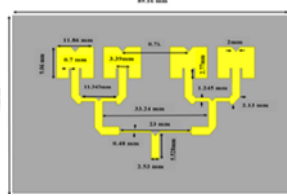
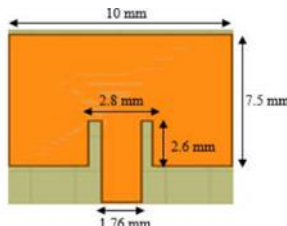
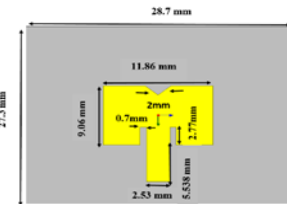


Figure 6. Comparison between single & 4-element patch array (a) S-parameter, (b) Radiation pattern, (c) Gain at 10 GHz.

It is clear from Fig.6 (c), the gain increases from 8 dB to 13.3 dB.

Table 1 shows a comparison between of the proposed antenna shown in Fig.1 to previously published similar designs in light of the most recent research. The data clearly shows that the proposed design, which can be either a single or four-element patch antenna with tuned dimensions, provides higher gain and a wider 10-dB bandwidth than previously reported [4-6].

Table 1 shows a comparison between the antenna model and earlier studies.

Publication	Shape of antenna	Frequency band	Central Frequency (GHz)	BW (MHz)	Gain dB
B. Yunia et. al., 2020 [4]		X-Band	10	410	10.94
Rahul et. al., 2018 [5]		X-Band	11.5	470	6
This work, 4- element patch array		X-Band	10	1200	13.3
N. C. Okoro & L. I. Oborkhale, 2021 [6]		X-Band	10	226.2	6.58
This work, one element patch antenna		X-Band	10	700	8

4. Application of the proposed antenna for Detecting Brain Tumor

Human tissue is a highly non-homogeneous material. Blood, fat, and a number of other biological components with varied permittivity and conductivity make up the body. At the antenna resonance frequency, Fig. 7 displays the head phantom model for acceptable tissue parameters such as permittivity and conductivity. The model is made up of seven layers of spherical forms, including skin, fat, Dura, bone, CSF, brain, and tumors at 10 GHz. Table 2 shows the dimensions of the planned phantom [12]. Tumors can be identified by approaching the proposed slotted patch antenna to the human head phantom model. The signal propagation from antenna to head model will be impacted due to the existence of tumor cells inside the brain tissue, and the variation in the matching and radiation characteristics can be easily captured and identified.

Table .2 Dimension and the dielectric characteristics of the spherical cancer head phantom around 10 GHz [12].

Tissue in order	Radius (mm)	Dielectric constant (ϵ_r)	Conductivity, σ (S/m)
Brain	81	43.22	1.29
CSF	83	70.1	2.3
Dura	83.5	46	0.9
Bone	87.6	5.6	0.03
Fat	89	5.54	0.04
Skin	90	45	0.73
tumor	5-10	55	7

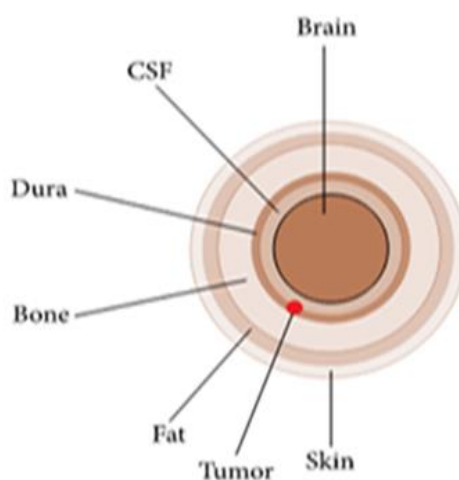


Figure 7. The proposed spherical tumor head phantom with tumor at 10 GHz [12].

The suggested DGS antenna and head phantom model are intended to be placed 4 mm apart from one another. An antenna's function is to deliver enough energy to penetrate human diseases. The proposed antenna has been used in two different versions of the brain phantom, one with and one without a tumor. The following discussion covers all of the simulation's determined results as seen in Figure 8.

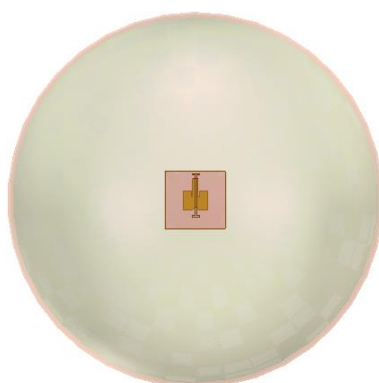


Figure 8. the proposed Microstrip Patch Antenna is designed to be put at a 4mm distance from the head phantom

The proposed antenna is placed at a distance of 4 mm from the head phantom. The return loss of the proposed MPA is calculated as shown in Fig.9. When the antenna was applied to brain phantoms that were cancer-free and cancer-affected, with cell sizes of 5 mm and 10 mm, the resonant frequencies is shifted as well as the 10-dB bandwidth is increased.

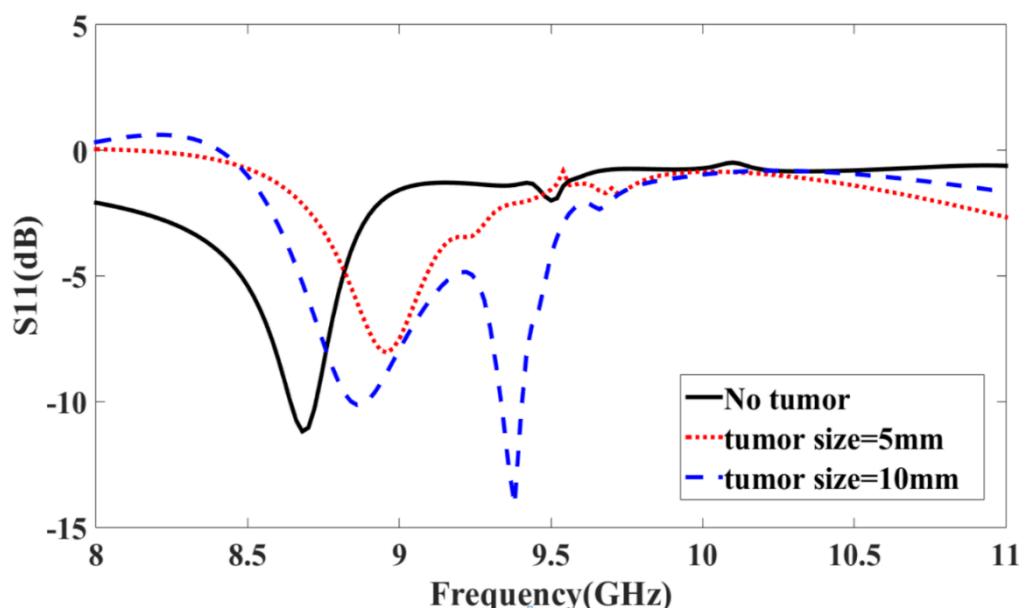


Figure 9. Detecting Brain Tumor Through calculating: Return loss (dB).

SAR is a metric that commonly used to describe the maximum permissible level of electromagnetic radiation that a communication antenna in a variety of wireless devices can produce. SAR is a measurement of the amount of electromagnetic energy deposited in human body tissue over time and can be calculated using the following relation [2].

$$SAR = \frac{\sigma}{\rho} [E]^2 = \frac{J^2}{\rho\sigma} [W/Kg] \quad (4)$$

where E is the rms value of the tissue's electric field strength [V/m], J is the current density [A/m], σ is the head tissue's conductivity [S/m], and ρ is the density of head tissues [kg/m³].

It is a crucial parameter that must be kept within a predetermined range. According to the ICNIRP and FCC recommendations, the IEEE C95.3-2002 standard sets the standard level of SAR and states that for one gramme of typical body tissue, the level of SAR cannot exceed 1.6 W/kg [2]. Microwave-based brain imaging devices' safety must be protected by a correct analysis of SAR, since even exposure for a short time to emission might pose a severe health risk. Calculating SAR can be applied to successfully detecting brain tumor.

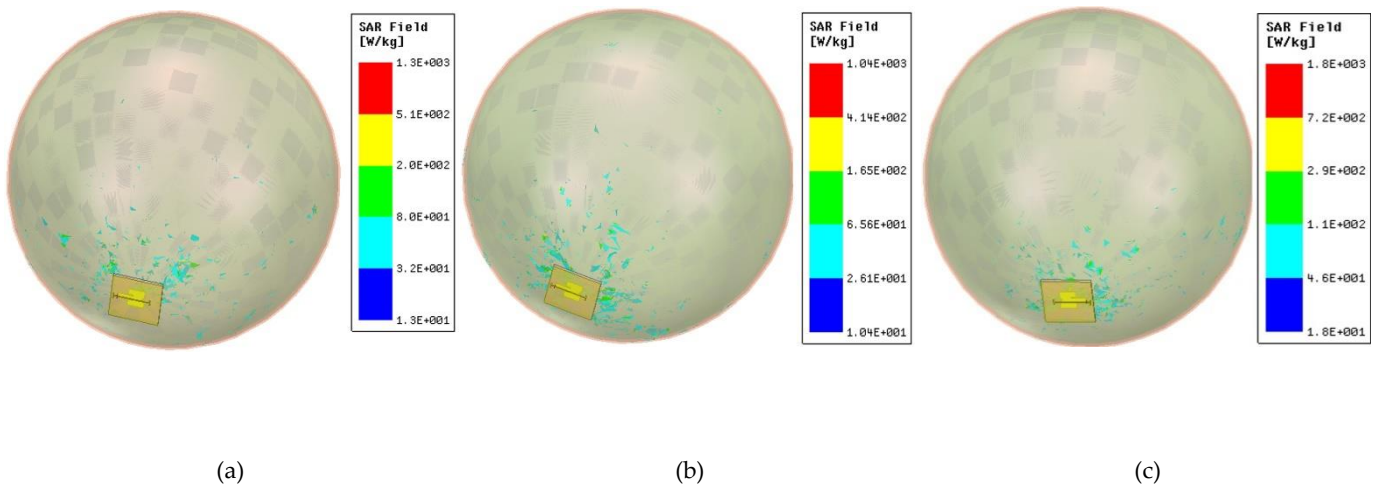


Figure 10. SAR versus tumor cell size. (a) No tumor, (b) cell size = 5 mm, (c) cell size = 10 mm at 10 GHz

The 10 GHz-captured SAR for the brains with and without tumor of various cell sizes is shown in Figure 10. The figure shows that for human tumor with radii of 5 mm and 0 mm, the highest SAR values are equal to 1.04 w/kg and 1.3 w/kg; respectively. The SAR for tumor with radius of 10 mm is 1.8 w/kg, which is higher than the average value of 1.6 w/kg. To ensure safe detection, the dimensions of the proposed antenna need to be maximized to have SAR values within standard limits. Figure 11 shows the proposed single patch design with rescaled dimensions by doubling the antenna's dimensions suggested in Fig.1 and thereby, the operating frequency will be around 5 GHz.

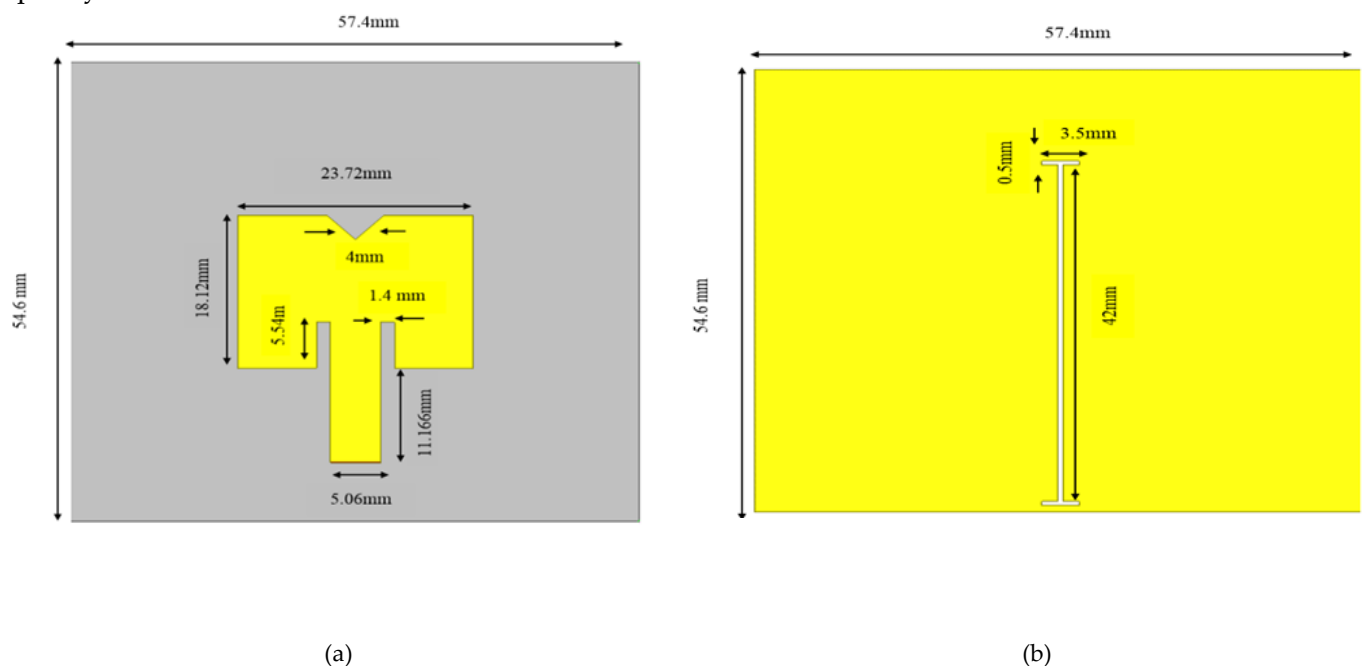


Figure 11. Proposed single patch design with rescaled dimensions (a) top view, (b) bottom view

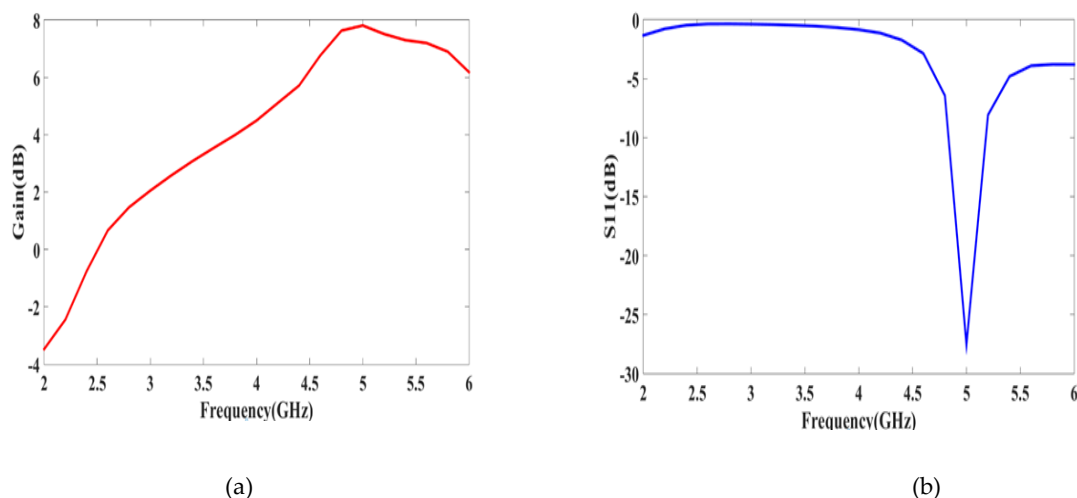


Figure 12. Gain and Return loss of proposed antenna

Figure 12 shows the calculated return loss and gain for the proposed antenna with scaled dimensions. It can be evident clearly from the figure that at around 5 GHz, S11 is equivalent to -27 dB, the bandwidth reaches 700 MHz, and the gain is constant at 8 dB. The single-patch DGS antennae that are being suggested are meant to be positioned 4 mm apart from the head phantom. Table 3 shows the dielectric characteristics of the spherical cancer head phantom around 5 GHz [14-15].

Table .3 The dielectric characteristics of the spherical cancer head phantom around 5 GHz [14-15].

Tissue	Dielectric constant (ϵ_r)	Tan δ
Skin	35.11	0.33
Fat	9.86	0.26
Bone	11	0.59
Dura	60.47	0.37
CSF	60.47	0.4
Brain	44	0.35

The calculated S11 curves for the proposed rescaled antenna set near the head model with and without Tumors are shown in Fig. 13. It is clearly shown in the figure that at 4.9 GHz, the tumor-free brain phantom managed to achieve an effective return loss of -16 dB. Both the head Phantom with the cancer cell size of 10 mm at resonant frequency of 5 GHz and the head Phantom with the cancer cell size of 5 mm at frequency of 4.6 GHz successfully acquired return losses of -19.6dB and -18.6dB, respectively.

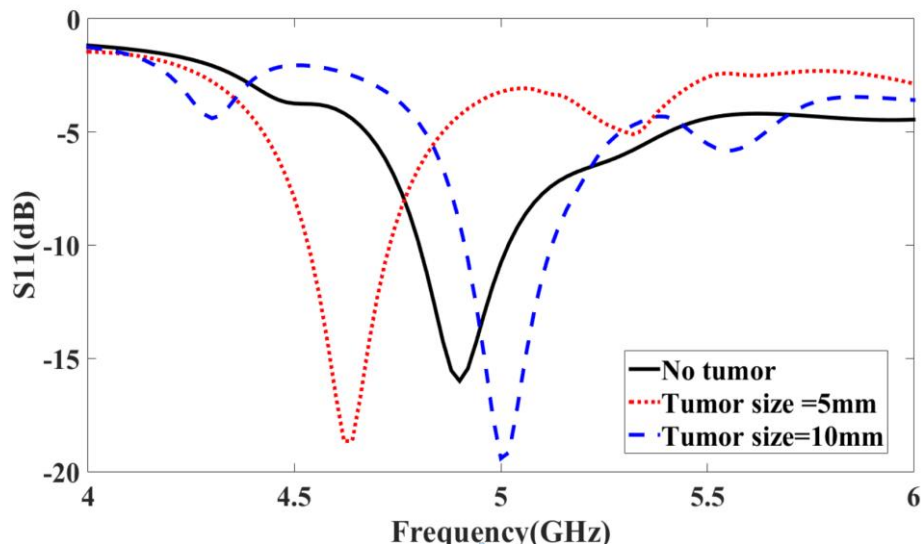


Figure 13. Return loss of Proposed antenna at frequency at 5GHz.

Additionally, the capability of the proposed antenna to detect tumors at different locations in the brain has been tested as shown in Fig. 14. The S_{11} results shown in Fig.15 show clearly that the proposed antenna can identify the tumors with radius of 5 mm located either at the center of the head model or at edge of the brain (40 mm from the center of the head model) where the average shift in the resonant frequencies in comparison with no tumor reads about 200 MHz. Figure 16 displays the SAR values of the head phantom with and without cancer. Here, a SAR value of 0.68W/kg was achieved using the antenna model on a brain phantom free of cancer. Using an antenna on a brain phantom with cancer that was 5 mm and 10 mm in size, respectively, we successfully recorded SAR values of 0.77 and 0.66 W/kg that are less than the industry standard of 1.6 W/kg. It should be obvious that increasing the size of the suggested antenna will lower its SAR value.



Figure 14. The head phantom with different location of tumor cell(a) No tumor (b) edge of the brain model and (c) center of the brain model.

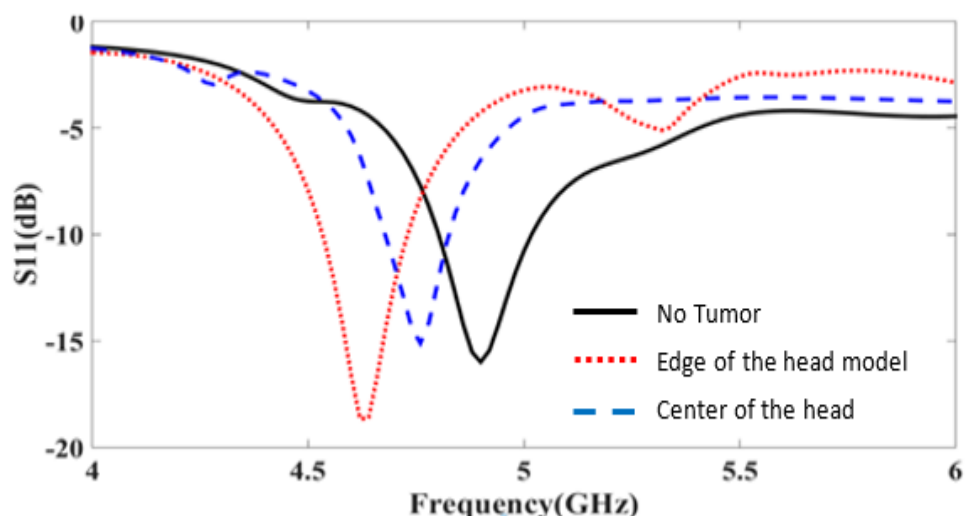


Figure 15. Return loss versus different location of tumor cell at 5GHz(a)return loss and gain

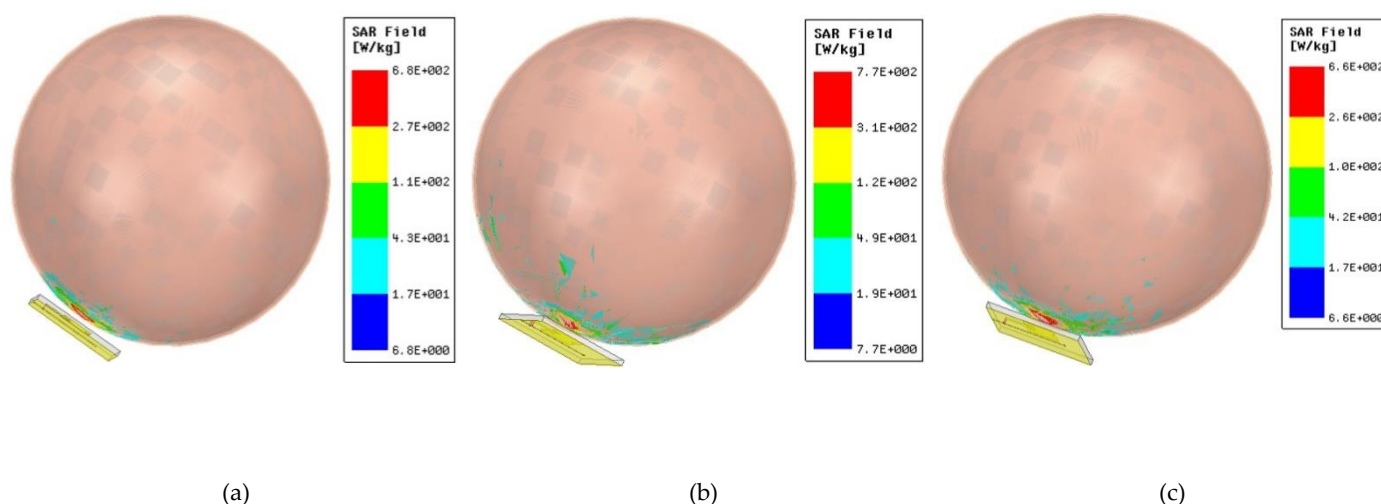


Figure16. SAR versus tumor cell size. (a)No tumor, (b) tumor size = 5mm and (c)tumor size = 10mm at the same location.

5. Conclusion

In order to find brain cancer in its earliest stages, this study's research led to the development of a rectangular microstrip patch antenna using DGS. Following the use of the Antenna in both the brain model of a healthy human brain and a brain model that has been harmed by a tumor, this work demonstrates a precise method for describing distinct tissues in various simulated scenarios. First, a human head phantom model was modeled. The designed antenna, which has 5 GHz operating frequency, was mounted on the head's phantom at a separation of 4 mm. When the antenna was applied to brain phantoms that were cancer-free and cancer-affected, with cell sizes of 5 mm and 10 mm, the resonant frequencies of the calculated return loss curves of the proposed antenna read 4.8, 4.8, 5 GHz; respectively. The SAR values of 0.77 W/kg and 0.66W/kg and 0.6W/kg were likewise attained after the antenna was used on brain phantoms with tumor size 5mm and 10mm and without tumors at 5GHz, respectively. It has been discovered from all the collected data that the suggested antenna is quite practical and suitable to find out if there is brain tumor or not.

References

1. Cardoso, V., Dinis, H. and Mendes, P.M., 2019, November. Electric Field Array Detector for Millimeter Wave Assistance on Brain Tumor Resection. In 2019 IEEE International Conference on Microwaves, Antennas, Communications and Electronic Systems (COMCAS) (pp. 1-4), 2019.
2. Raihan, R., Bhuiyan, M.S.A., Hasan, R.R., Chowdhury, T. and Farhin, R., 2017, August. A wearable microstrip patch antenna for detecting brain cancer. In 2017 IEEE 2nd International Conference on Signal and Image Processing (ICSIP) (pp. 432-436), 2017.
3. Chowdhury, T., Farhin, R., Hassan, R.R., Bhuiyan, M.S.A. and Raihan, R., 2017, September. Design of a patch antenna operating at ISM band for brain tumor detection. In 2017 4th International Conference on Advances in Electrical Engineering (ICAEE) (pp. 94-98), 2017.
4. Bidadariana Yunia Utami Putri's, Eka Setia Nugraha , Anantia Prakasa "Design and Performance Analysis of Linear Array Microstrip Antennas with Mitered-Bends Feeding Network for X-Band Radar Applications", Jurnal Elektronika dan Telekomunikasi (JET) Vol. 20, No. 1, pp. 9-15, August 2020.
5. Dr. Rahul G. Mapari ,Rahul S. Parbat, "Design of 4X1 Microstrip Array Antenna for X-Band Satellite Communication Application". International Journal of Pure and Applied Mathematics Vol. 118 No. 24 2018
6. N. C. Okoro & L. I. Oborkhale," Design and Simulation of Rectangular Microstrip Patch Antenna for X-Band Application", Global Journal of Researches in Engineering vol 21, no 3, 2021
7. C. A. Balanis, Antenna Theory Analysis and Design, 4th ed. New York: Wiley, 2016
8. Kahwaji, A., Arshad, H., Sahran, S., Garba, AG and Hussain, R.I., 2016, March. Hexagonal microstrip antenna simulation for breast cancer detection. In 2016 International Conference on Industrial Informatics and Computer Systems (CIICS) (pp. 1-4), DOI:10.1109/ICCSII.2016.7462400
9. Rokunuzzaman, M., Samsuzzaman, M. and Islam, M.T., 2016. Unidirectional wideband 3-D antenna for human head-imaging application. IEEE Antennas and Wireless Propagation Letters, 16, pp.169-172..
10. J H. Zhang, A. O. El-Rayis, N. Haridas et al., "A smart antenna array for brain cancer detection," in Proceedings of the Loughborough Antennas & Propagation Conference, pp. 1-4, Loughborough, UK, 2011.
11. J M. F. Abedin, M. Z. Azad, and M. Ali, "Wideband smaller unit-cell planar EBG structures and their application," IEEE Transactions on Antennas and Propagation, vol. 56, no. 3, pp.903-908, 2008..
12. Reefat Inum , Md. Masud Rana, Kamrun Nahar Shushama, and Md. Anwarul Quader, "EBG Based Microstrip Patch Antenna for Brain Tumor Detection via Scattering Parameters in Microwave Imaging System" International Journal of Biomedical Imaging, Vol, Article ID 8241438, 12 pages .
13. Radouane Karli, Hassan Ammor, "A WIFI antenna radiation effects on human head in the ISM Band", Journal of Emerging Technologies in Web Intelligence, vol. 6, no. 01, pp. 45-48. 2014..
14. Abdul Rashid O. Mumin, R. Alias, Jiwa Abdullah and S.H. Dahlan, "3Design a compact square ring patch antenna with AMC for SAR reduction in WBAN applications," Bulletin of Electrical Engineering and Informatic, vol.9, No.1 February 2020.
15. Dielectric properties of body tissues in the frequency range 10 Hz to 100 GHz, Available at: <http://niremf.ifac.cnr.it/tissprop/>, June 10th, 2014.
16. Demyana A. Saleeb, Rehab M. Helmy, Nihal F. F. Areed, M. Marey, Wazie Abdulkawi and A. Elkorany, " A Technique for the Early Detection of Brain Cancer Using Circularly Polarized Reconfigurable Antenna Array," IEEE Access, vol 9, 2021
17. Demyana A. Saleeb, Rehab M. Helmy, Nihal F. F. Areed, M. Marey, Wazie Abdulkawi and A. Elkorany, " Detection of Kidney Cancer Using Circularly Polarized Patch Antenna Array," IEEE Access, vol. 10, 2022.